Fluctuation Effects on a Strongly Pinned Vortex Lattice in a Thin Type-II Superconducting Wire

X. S. Ling,* J. D. McCambridge, N. D. Rizzo,† J. W. Sleight, and D. E. Prober
Department of Applied Physics, Yale University, New Haven, Connecticut 06520-8284

L. R. Motowidlo and B. A. Zeitlin
IGC Advanced Superconductors, Inc., Waterbury, Connecticut 06704
(Received 17 October 1994)

We report on transport properties of the vortex lattice in fine, round NbTi wires fabricated by a novel wire-drawing process. The voltage onset in the isothermal I-V characteristic is sharp for thick wires ($d \geq 1$ μm) at 4.2 K and 6 T, but is rounded for thinner wires. The thinnest wires also display an Ohmic resistivity at low current densities. This linear resistivity decreases exponentially with temperature near $T_c(H)$ and approaches a constant value at low temperatures. We explain our results as finite size effects of the thermal and quantum collective creep of vortex lines.

PACS numbers: 74.60.Ge, 74.40.+k

Larkin showed [1] two decades ago that random pinning in type-II superconductors always destroys the long-range translational order in the vortex lattice. The statics and dynamics of a pinned vortex lattice are governed by a three-way competition between vortex-vortex interactions, vortex-pin interactions (quenched pinning disorder), and thermal fluctuations. Anderson pointed out [2] that vortex-vortex interactions must play a role in the dynamics of vortex motion. He suggested that such interactions lead to "bundles" of moving vortex lines. Nevertheless, it was believed [2,3] that one could treat the bundles as noninteracting particles moving in a washboard-type pinning potential. In this classical flux creep picture, the vortex-pin interaction dominates the dynamical behavior. Since the intrinsic pinning potential is always finite, this classical picture leads to a finite Ohmic resistivity for $T > 0$ in the pinned vortex state [3]. Feigel'man *et al.* [4] extended Anderson's original vortex bundle idea further to include the interactions between the bundles. As a result, the depinning bundle size—hence the energy barrier—grows infinitely as the driving force is reduced [4]. Thus, the Ohmic resistivity of a bulk sample in the pinned vortex state is zero. Using a symmetry-breaking argument, Fisher argued [5] that this pinned vortex state is a new thermodynamic phase, a vortex glass. He postulated [5] that there is a new superconducting phase coherence in the pinned vortex state, even though quenched pinning disorder destroys the translational order of the vortex state.

To understand this phase coherence in the pinned vortex state, it is helpful to recall studies of the Meissner superconducting state ($B = 0$) in one-dimensional (1D) wires [6–8]. Fluctuation effects interrupt the phase coherence in these wires. A Langer-Ambegaokar nucleation argument [6] leads to an energy barrier to phase slippage which is proportional to the cross-sectional area of the wire. Thus, it is only possible to study the fluctuation effects in very thin wire samples. It is now well established theoretically [6] and experimentally [7] that thermally activated phase slippage leads to broadening of the zero-field resistive transition in a 1D superconducting wire. Well below T_c, there is compelling experimental evidence [8] that the thermally activated process gives way to a quantum tunneling process. We show in this Letter that, for narrow wires, there is a strong similarity between the fluctuations of phase coherence in the Meissner state and the fluctuations of the new phase coherence in the vortex glass state.

We describe here an experiment on type-II superconducting wires, with diameters varying from 100 to 0.06 μm. The starting superconducting material was annealed high-homogeneity grade Nb–46.5 wt.% Ti alloy [9]. We chose this alloy because of its high ductility and the availability of ample data on its metallurgical and superconducting properties [10]. The materials parameters of this alloy are $\rho_n \approx 70$ $\mu\Omega$ cm, $T_c \approx 9$ K, $\xi(4.2\text{ K}) \approx 5$ nm, and $\lambda(4.2\text{ K}) \approx 280$ nm. We produced samples by bundling a Cu-clad NbTi rod with 60 pieces of pure Nb rod [11] in a Cu tube. The 61 rods formed a hexagonal array with the NbTi in the center. Using a draw bench, we reduced the diameter of this billet by a factor of 9, then cut the wire into another 61 pieces and again restacked the rods inside a copper tube. After drawing, restacking, and drawing the wire once more, we had reduced the diameter of the NbTi rods to submicron size while maintaining a macroscopic total wire diameter. No heat treatments were used for our wires, in contrast to the production of commercial NbTi magnet wire. Thus, the bulk critical current density of our filaments, $J_c \sim 2 \times 10^4$ A/cm^2 at 4.2 K and 6 T, is an order of magnitude smaller; the pinning is primarily by grain boundaries [10].

Though the pinning in our filaments is weaker than that of commercial NbTi wire, we still find that our samples are in the strong pinning regime. Using the bulk value for J_c at 6 T and 4.2 K, we estimated the Larkin

pinning length [12] in our cold-drawn NbTi, $R_c \sim (C_{66}\xi/J_cB)^{1/2} \sim 20$ nm $\sim a$ (the flux lattice unit cell). $C_{66} = (B_{c2}^2/4\pi)(1 - 1/2\kappa^2)b(1 - b)^2(1 - 0.29b)/8\kappa^2$ and $C_{44} = B^2/4\pi$ (see below) are the shear and tilt (local limit) moduli of the vortex lattice, where $b = B/B_{c2}$. Since C_{66} is expected to be reduced for the narrow wire geometry [13], the above estimate for R_c is an upper bound. Thus, the vortices in the as-drawn NbTi wires are in an amorphous, or strong pinning, state by the definition of Larkin and Ovchinnikov [12]. In the classical Anderson-Kim picture, the energy barrier for flux creep is mainly determined by the strength of pinning. Even though NbTi is a strong pinning, low-T_c material, we show below that fluctuation effects are significant in very thin wires.

Each filament in the final wire consists of a NbTi core with a thin layer of Cu and a thick Nb jacket. Figure 1(a) shows a scanning electron micrograph (SEM) of the cross section of a typical multifilamentary wire. The nearly round shape of the NbTi core is shown in a closeup in Fig. 1(b). After etching away the thick Cu matrix, we placed individual filaments on a silicon substrate. We used Ag paint to make electrical contacts (standard four-point measurement) with the current leads well away from the voltage probes to eliminate erroneous current-transfer voltage [14]. Typical contact resistance was less than 1 Ω. Each filament was examined using a SEM to ensure uniformity of the diameter over its entire length. We made the 4.2 K measurements with the sample immersed in liquid helium; we made the temperature dependent measurements with a standard variable temperature cryostat. To ensure that there were no self-heating effects, we compared I-V curves taken in vacuum and in the bath. We also found no evidence of hysteresis in traces where the current was swept up past I_c and back down to zero.

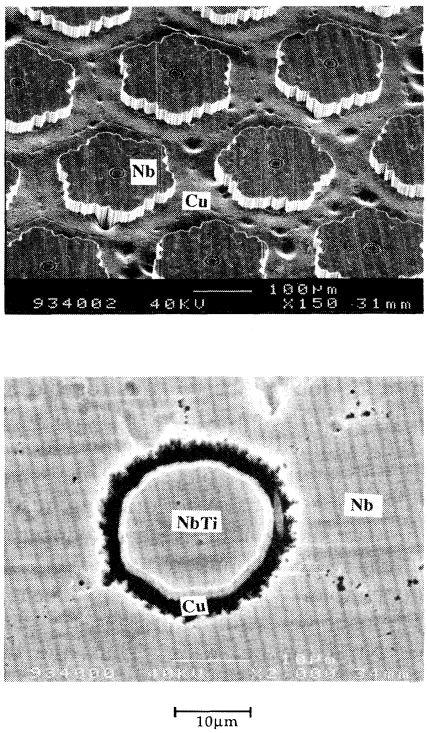

FIG. 1. SEM micrograph showing the structure of a superconducting NbTi filament: (a) multifilaments of Nb-clad NbTi cores in a Cu matrix, the Cu matrix outside the Nb jacket will be etched away so that each filament can be measured individually; (b) close-up view of the NbTi core.

At 4.2 K and 6 T, for NbTi core diameters greater than 1 μm, the voltage had a sharp onset. B was oriented perpendicular to the wire. As we reduced the diameter of the core below 1 μm, the voltage onset in the I-V curves became rounded. As we reduced the diameter of the core below ~0.3 μm, an Ohmic resistivity appeared at low current densities. In Fig. 2, we plot electric field E vs current density J for four NbTi filaments with core diameters 1.50, 0.57, 0.32, and 0.12 μm, at $B = 6$ T and $T = 4.2$ K.

Behavior similar to Fig. 2 was observed recently at 4.2 K in narrow strips of Nb film of intermediate width [15] and in fine NbTi filaments with artificially engineered pinning centers [16]. However, a low current Ohmic resistivity is not observed in multifilamentary wires with fine subfilaments [16]. This behavior can be explained successfully as an effect of thermally activated collective creep in a small sample: The depinning bundle size is limited by the dimensions of the sample [15,16]. In general, a depinning bundle has a volume $R_\perp R_\parallel L \sim R_\perp R_\parallel^2$, and $L \sim R_\parallel \gg R_\perp$; $R_\perp$, $R_\parallel$, and L are bundle sizes transverse to the direction of hopping (along the wire), along the direction of hopping (across the wire), and along the field (normal to the wire). The energy barrier U to depin this bundle is $C_{66}(\xi/R_\perp)^2 R_\perp R_\parallel^2$ [4]. Once $R_\parallel$ is larger than the sample diameter, $R_\parallel$ is replaced by d, and $U \sim C_{66}(\xi/R_\perp)^2 R_\perp d^2$. Thus, in real samples, the Ohmic resistivity for $T > 0$ is always finite because

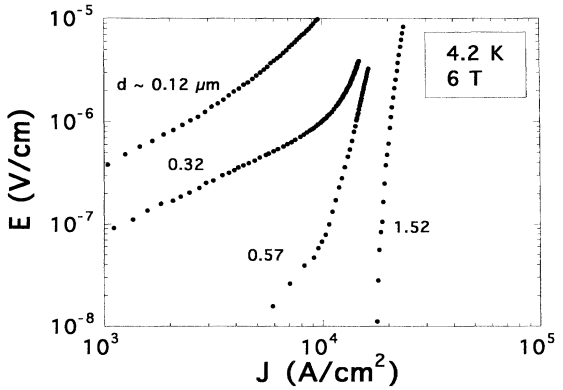

FIG. 2. Current-voltage characteristics for filaments with various diameters. The current density is calculated from the cross-sectional area of the NbTi core.

the energy barrier is finite. Only in very thin wires, however, is this finite resistivity detectable. Previous work examined this low current Ohmic resistance over a limited temperature range [15,16]. In this Letter, we study the origins of these fluctuation effects in a much larger temperature range.

We measured I-V curves at various fixed temperatures for filaments with different diameters. We find that the low current tails of the I-V curves remain linear even for temperatures well below $T_c(B)$. Figure 3 is an Arrhenius plot of the Ohmic resistivity data. The area we used for converting resistance to resistivity is that of the NbTi core. The correction due to the thick Nb jacket is negligible below 5×10^{-9} Ω cm. The level-off of resistivity above $\sim 10^{-8}$ Ω cm represents the resistive shunt by this Nb jacket; the normal-state resistivity of NbTi is $\sim 10^{-4}$ Ω cm. Therefore, the onsets of the transitions (Fig. 3) occur after the resistivity of the NbTi core has already dropped by 4 orders of magnitude from its normal-state value. The resistivity is thermally activated near the transition, but becomes nearly independent of temperature far below the transition.

We also studied the field dependence of the resistive transition in the thin filaments with a lock-in amplifier (PAR 124). The ac current level (35 nA at 3 kHz) was low enough so that the measurement was in the Ohmic regime; this was verified independently by dc I-V traces. Figure 4 is an Arrhenius plot of the resistive transition for a wire (normalized to the normal-state value) with a diameter of 0.083 μm, in fields of 0.5, 1, 2, 3, 4, 5, and 6 T (from left to right). The lines are fitting curves of a thermal-activation formula: $R/R_n = \exp(-U/k_BT)$, and $U = U(B,d)[1 - T/T_c(B)]^{3/2}$ with $U(B,d)$ and $T_c(B)$ as two fitting parameters. The extracted field dependence of U is shown in the inset of Fig. 4. We found $T_c(B)$ was linear with slope $dB/dT = -2.35$ T/K. We also tested other values for the exponent of the $1 - T/T_c(B)$ term, but the power $\frac{3}{2}$ gave the most satisfactory fit. It is interesting to point out that the temperature and field dependences of the activation energy resemble those of Tinkham [3].

We have made three important improvements in this experiment over previous work: the Nb jacket and round NbTi core remove the surface barrier found by Ando *et al.* [15]; the jacket eliminates self-heating problems [17]; and the density of pinning centers (primarily grain boundaries) is nearly constant for all our present samples [18]. With these improvements, we are able to observe clearly the finite-size effect of the collective creep down to very small wire diameters. The energy barrier extracted from the thermally activated region of the resistive transition curve, as in Fig. 3, is approximately proportional to the area of the core ($\sim d^2$). For the $d = 0.32$ μm core at 6 T, $U(B,d) \sim 200$ K. This agrees well with a simple estimate [16] using the collective creep model. The small sample size leads to a small energy barrier. This greatly reduced energy barrier allows the observation of additional fluctuation effects: From Figs. 3 and 4, it is clear that there is a crossover from a thermally activated process to a nonthermal mechanism as temperature is reduced far below T_c.

Our size and temperature dependent resistance data in Fig. 3 are reminiscent of the data of Giordano [8] on 1D superconducting wires. There also, the additional dissipation well below T_c was only observable in 1D wires with diameters of a few hundred angstroms [8]. Giordano [8] has suggested that phase slips due to macroscopic quantum tunneling may be the cause of the low temperature resistance tail in the 1D wires he studied in zero field. One possible mechanism for our low

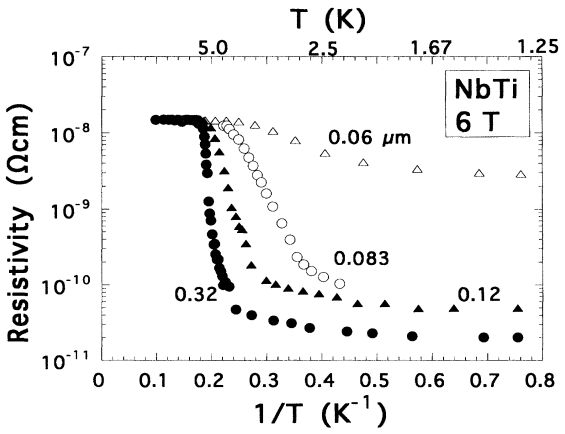

FIG. 3. Low current Ohmic resistivity as a function of temperature for various wire diameters. Each data point on this figure is from a full I-V trace.

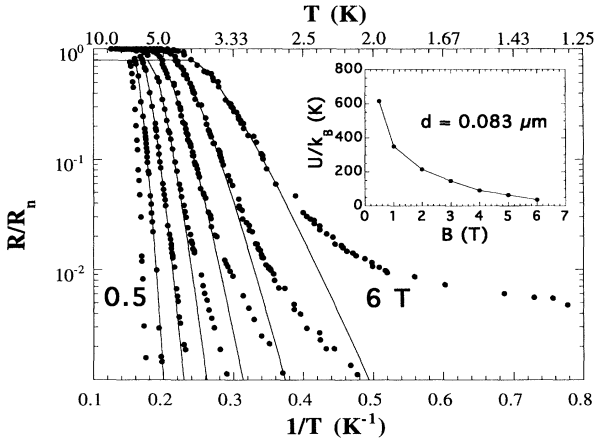

FIG. 4. Arrhenius plot of the resistive transition of a wire ($d = 0.083$ μm) in various fields. Above the line at $R/R_n \sim 0.8$, the shunt resistance of the Nb cladding becomes important. The data above this line were not used for fitting. Inset: temperature-independent part of $U, U(B,d)$ vs B, see text.

temperature resistivity tail could be quantum tunneling of vortices through the energy barrier [19]. One expects a crossover from thermal activation to quantum tunneling to occur when $U/k_BT \sim S_{\rm eff}/\hbar$, where $S_{\rm eff} = \tau U$ is the effective action, and τ is the tunneling time for a vortex bundle to escape through the barrier. The crossover temperature $T_* \sim \hbar/\tau k_B$ is expected to be *independent* of the wire size for 1D superconductors in the Meissner state [8]. From Fig. 3, one can see that T_* does depend on the wire size in our case. This indicates that the tunneling time τ has to be related to the sample size. One can understand this behavior qualitatively from the theory of quantum collective creep [19]. In quantum creep theory, the tunneling time of a vortex bundle is $\tau \sim R_\perp^2 \eta/a^2 C_{66}$, where η is the viscosity. For an elastic deformation, $R_\perp \sim (C_{66}/C_{44})^{1/2} R_\parallel$. $R_\parallel$ is replaced by d if $R_\parallel$ exceeds d. Thus $R_\perp$—hence τ—will depend on d. The full details of these relations are unknown at this stage. It is therefore difficult to compare our data quantitatively with the present theories of quantum creep of vortices developed for bulk samples. We hope that our result will stimulate theoretical work on quantum collective creep in the regime of our experiment.

Our data seem to agree qualitatively with the theory of quantum creep. However, it is somewhat difficult to imagine the quantum tunneling of several vortices simultaneously through an energy barrier. To gain further insight into this problem, it is helpful to go back to Fisher's original phase coherence argument [5] for the vortex glass. He argued [5] that a pinned disordered vortex lattice possesses a new *superconducting* phase coherence. By analogy to the original superconducting phase coherence of the Meissner state, the new phase coherence in a narrow filament can only be interrupted by phase slippage. Just as phase slippage in the Meissner state involves many Cooper pairs, phase slippage in the pinned vortex state might involve many vortices. It is therefore possible to have a single phase slippage event involving several vortices in a quantum mechanical tunneling process. Thus, there appears to be a profound relationship between the new Fisher phase coherence in a pinned vortex lattice and quantum tunneling of several vortices simultaneously.

We gratefully acknowledge helpful discussions with Paul Chaikin, Shobo Bhattacharya, and David Larbalestier. This work was supported by the Connecticut Department of Economic Development, Grant No. 92G036, by the Intermagnetics General Corporation, and by NSF Grant No. DMR-9112752.

* Present address: NEC Research Institute, Princeton, NJ 08540.
† Also at Department of Physics, Yale University.

[1] A. I. Larkin, Sov. Phys. JETP **31**, 784 (1970).
[2] P. W. Anderson, Phys. Rev. Lett. **9**, 309 (1962); P. W. Anderson and Y. B. Kim, Rev. Mod. Phys. **36**, 39 (1964).
[3] M. Tinkham, Phys. Rev. Lett. **61**, 1658 (1988).
[4] M. V. Feigel'man, V. B. Geshkenbein, A. I. Larkin, and V. M. Vinokur, Phys. Rev. Lett. **63**, 2303 (1989).
[5] M. P. A. Fisher, Phys. Rev. Lett. **62**, 1415 (1989).
[6] J. S. Langer and V. Ambegaokar, Phys. Rev. **164**, 498 (1967); D. E. McCumber and B. I. Halperin, Phys. Rev. B **1**, 1054 (1970).
[7] J. E. Lukens, R. J. Warburton, and W. W. Webb, Phys. Rev. Lett. **25**, 1180 (1970); R. S. Newbower, M. R. Beasley, and M. Tinkham, Phys. Rev. B **5**, 864 (1972); M. Tinkham, *Introduction to Superconductivity* (Robert E. Krieger Publishing, Malabar, FL, 1980), pp. 230–237.
[8] N. Giordano, Phys. Rev. B **43**, 160 (1990); **41**, 6350 (1990).
[9] Teledyne Wah Chang Albany, P.O. Box 460, Albany, Oregon 97321.
[10] E. W. Collings, *A Sourcebook of Titanium Alloy Superconductivity* (Plenum Press, New York, 1983).
[11] Nb rods were used because of their metallurgical compatibility with NbTi and Cu. In our experiment, the magnetic fields are larger than the upper critical field (~1 T at 4.2 K) of heavily cold-worked Nb. Thus the Nb jacket is a normal-metal cladding.
[12] A. I. Larkin and Yu. N. Ovchinnikov, J. Low Temp. Phys. **34**, 409 (1979).
[13] E. H. Brandt, J. Low Temp. Phys. **42**, 557 (1981).
[14] J. E. Ekin, J. Appl. Phys. **49**, 3406 (1978).
[15] Y. Ando, H. Kubota, S. Tanaka, M. Aoyagi, H. Akoh, and S. Takada, Phys. Rev. B **47**, 5481 (1993); Y. Ando, H. Kubota, and S. Tanaka, Phys. Rev. B **48**, 7716 (1993).
[16] X. S. Ling, J. D. McCambridge, D. E. Prober, L. R. Motowidlo, B. A. Zeitlin, and M. S. Walker, Physica (Amsterdam) **194–196B**, 1867 (1994).
[17] W. J. Skocpol, M. R. Beasley, and M. Tinkham, J. Appl. Phys. **45**, 4054 (1974).
[18] A. W. West and D. C. Larbalestier, Metall. Trans. A **15A**, 843 (1984).
[19] G. Blatter, V. Geshkenbein, and V. M. Vinokur, Phys. Rev. Lett. **66**, 3297 (1991); B. I. Ivlev, Y. N. Ovchinnikov, and R. S. Thompson, Phys. Rev. B **44**, 7023 (1991).

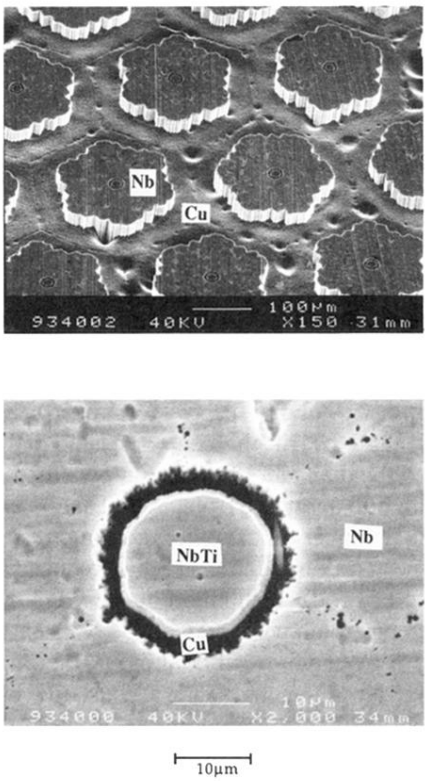

FIG. 1. SEM micrograph showing the structure of a superconducting NbTi filament: (a) multifilaments of Nb-clad NbTi cores in a Cu matrix, the Cu matrix outside the Nb jacket will be etched away so that each filament can be measured individually; (b) close-up view of the NbTi core.